LAWRENCE
LIVERMORE
NATIONAL
LABORATORY

LLNL-CONF-655061

System for Calibrating the Energy-Dependent Response of an Elliptical Bragg-Crystal Spectrometer

R. E. Marrs, G. V. Brown, J. A. Emig, R. F. Heeter

May 29, 2014

20th Topical Conference on High Temperature Plasma Diagnostics
Atlanta, GA, United States
June 1, 2014 through June 5, 2014

Disclaimer

System for calibrating the energy-dependent response of an elliptical Bragg-crystal spectrometer[a)]

R.E. Marrs, G.V. Brown, J.A. Emig, and R.F. Heeter[b)]

Lawrence Livermore National Laboratory, Livermore, CA 94551, USA

(Presented XXXXX; received XXXXX; accepted XXXXX; published online XXXXX)
A multipurpose spectrometer (MSPEC) with elliptical crystals is in routine use to obtain x-ray spectra from laser produced plasmas in the energy range 1.0 – 9.0 keV. Knowledge of the energy-dependent response of the spectrometer is required for an accurate comparison of the intensities of x-ray lines of different energy. The energy-dependent response of the MSPEC has now been derived from the spectrometer geometry and calibration information on the response of its components, including two different types of detectors. Measurements of the spectrometer response with a laboratory x-ray source are used to test the calculated response and provide information on crystal reflectivity and uniformity.

I. INTRODUCTION

X-ray spectroscopy provides important information on the temperature, density, composition and other properties of laser-produced plasmas.[1] A current need is to extend prior benchmark data for gold plasmas in hohlraums.[2] Typically, x-ray spectra are measured with Bragg-crystal spectrometers, which may be coupled to different types of detectors. In the absence of a calibration of the energy-dependent response of the spectrometer, measurements can still provide important information on the structure of the x-ray spectrum, the presence or absence of specific charge states (line features), and transmission spectra when the backlighter and absorption spectra are recorded on the same detector and no cross-normalizations are required. However, to obtain relative and/or absolute measurements of x-ray intensity of different spectral features, knowledge of the energy-dependent spectrometer response is required.

A multipurpose Bragg-crystal spectrometer (MSPEC) was developed at LLNL,[3] and configurations with elliptical crystals[4] are frequently used to diagnose laser-produced plasmas. The MSPEC is used with gated microchannel-plate (MCP) framing cameras, x-ray film, image plates, and CCD detectors. Similar spectrometers have been constructed elsewhere and for other purposes.[5] The MSPEC's elliptical crystal geometry provides broad spectral coverage, makes the instrument's energy resolution insensitive to source broadening from the mm-size sources typical of laser produced plasmas,[4] and allows background (fluorescence) rejection at the second crossover focus behind the crystal. However the response of an elliptical-crystal MSPEC spectrometer typically varies by more than an order of magnitude over its energy range, due to the reflectivity and curvature of the crystal, the energy-dependent response of the detector, and the transmission of filters. This has some value in a broadband instrument, where greater sensitivity at higher photon energy (where plasma x-ray emission is typically weaker) can balance out signal levels across the spectrum. But it increases the challenge in obtaining a full, relatively calibrated spectrum. This work reports calculations and measurements of the MSPEC's energy-dependent response for several different configurations.

[a)]Contributed paper published as part of the Proceedings of the 20th Topical Conference on High-Temperature Plasma Diagnostics, Atlanta, Georgia, June, 2014.
[b)]Author to whom correspondence should be addressed: heeter1@llnl.gov

II. MSPEC GEOMETRY

The geometry of the MSPEC is shown in Fig. 1. The curved crystal follows the contour of an ellipse, with one focus at the x-ray source and the other near the detector plane. X-ray paths cross at the second focus. The crystal is flat in the transverse (non-Bragg) dimension. To maximize versatility, MSPEC uses standard existing planar detectors oriented perpendicular to, and centered on, the "line of sight" to the source.[3,4] The "line of sight" refers to the center line of the MSPEC hardware, which is the same as the center line of the diagnostic ports at the laser facilities where it is used. The axis of the crystal ellipse is offset from the line of sight in the dispersion direction. This allows the Bragg range to be varied further, and also enables a thick forward shield to block the detector from direct "straight through" illumination by the x-ray source. The detector is also protected against fluorescence and other backgrounds from the crystal, substrate and spectrometer housing, by an aperture placed near the second "crossover" focus of the crystal ellipse. In the nondispersive direction, perpendicular to the plane of Fig.1, x-rays diverge from a "space-resolving" imaging slit near the source, or from the source itself if no slits are used.

The MSPEC has been used with three different ellipse configurations, denoted E1, E2, and E3. Only the E1 configuration has been previously reported.[4] MSPEC-E1, -E2 and -E3 differ in the eccentricity of the ellipse, the angle of the ellipse's axis with respect to the instrument line of sight, and the particular segment of the ellipse on which the crystal is placed. Individual ray paths vary with each ellipse, but the standoff distance, from the x-ray source to the detector plane along the line of sight, is the same for all configurations. The MSPEC can be used with any crystal that can be bent and mounted on the elliptical substrates; CsAP, RbAP and PET are most frequently used. The present work considers the E1 geometry with PET crystals and the E3 geometry with CsAP crystals. The parameters

TABLE I. Parameters for 3 different MSPEC ellipses. *f* is the distance between the two foci, *e* is the eccentricity, η is angle between the ellipse axis and the spectrometer center line (i.e., line-of-sight), θ shows the Bragg angle range corresponding to detector impact positions of ±15 mm from the spectrometer center line, and E_x is the corresponding x-ray energy range for PET and CsAP crystals in eV. (The detectors used all have over 30 mm of active length.) The distance from the source to the detector plane is 381 mm. (See Fig. 1.)

Ellipse	*f* (mm)	*e*	η (degrees)	Θ (degrees)	E_x (PET)	E_x (CsAP)
E1	348	0.9885	4.6	14.1 - 28.7	2956 - 5807	1006 - 1977
E2	331	0.9914	5.4	12.6 - 24.2	3459 - 6484	1177 - 2207
E3	310	0.9950	5.2	8.8 - 18.4	4483 - 9280	1526 - 3159

of the three ellipse geometries and the energy ranges for these two different crystals are listed in Table I.

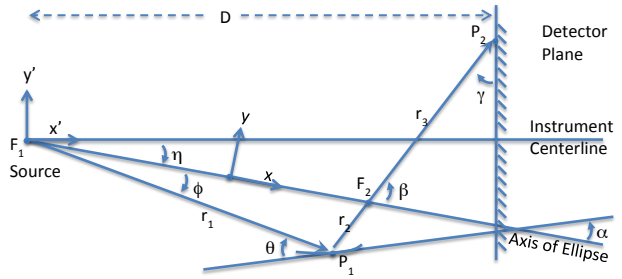

FIG. 1. MSPEC Geometry. X-rays propagate along r1 from source at F1 to crystal, Bragg scatter at P1, follow r2 through second focus F2, and propagate along r3 to hit the detector at P2. D = 381 mm is a fixed distance from source to detector plane. η is the angle between ellipse axis and instrument centerline, θ is the Bragg angle, γ is the complement of the detector incidence angle, and other angles are labeled for completeness. (x,y) and (x',y') define coordinate axes useful in geometric calculations for the ellipse and the instrument. The drawing is expanded vertically for clarity.

III. CALCULATED MSPEC RESPONSE

The energy-dependent response or sensitivity of the MSPEC spectrometer is a product of several different factors, including properties of the crystal and detector. The detector most often used with the MSPEC is a gated MCP framing camera with a phosphor anode and photographic film for recording the image. In this case, the phosphor light intensity per unit area is related to the source x-ray emission through the equation:

$$I = k\,S\,T\,R\,\frac{dE}{d\theta}\,\frac{d\Omega}{dA}\,M\,P\,F \qquad (1)$$

Here k is an unknown constant determined by the MCP gain and phosphor efficiency, S is the x-ray source emission in eV/sr/eV, and T is the filter transmission. The next three terms are properties of the crystal: R is the crystal integrated reflectivity in mr, and may be different for bent crystals than tabulated data for flat crystals; θ is the Bragg angle and dE/dθ is the derivative of Bragg's law which relates the photon energy range dE to the corresponding range of incident angles (in mr) at the crystal; and dΩ/dA is the solid angle per unit area on the detector, which is described in more detail below. The last three terms are properties of the detector (using an MCP here): M is the energy-dependent photoelectric efficiency of the MCP; P is the relative efficiency of the MCP as a function of the angle between the incident x-ray direction and the axis (pore angle) of the MCP channels; and F is the relative position-dependent flat-field response of the gated MCP, which is itself a function of the strip-to-strip timing for the 4-strip MCPs at large laser facilities.[6] The units used here are eV, mm, milliradians (mr), and steradians (sr). All quantities are direct or indirect functions of photon energy E. The "MSPEC response" here refers to all the terms on the right hand side of Eq. 1 except for the source emission S.

If the MSPEC response is known, it can be unfolded from the measured image intensity to obtain the source emission spectrum S. All of the terms in Eq. 1 have been calculated from available information and the geometry of the spectrometer. The filter transmission T is calculated from information in the CXRO database,[7] with filters of interest being calibrated more carefully using an electron beam ion trap[8] or synchrotron light source. The next three terms are properties of the curved crystal; they are collectively referred to as the crystal response G(E):

$$G(E) = R\,\frac{dE}{d\theta}\,\frac{d\Omega}{dA}\ \text{eV-sr/mm}^2 \qquad (2)$$

The integrated reflectivity R is taken from information in the literature,[11] but it is not well known for CsAP, and it is affected by crystal quality and crystal bending. The tabulated reflectivity of a perfect crystal can be an order of magnitude different from that of a mosaic crystal. This fundamental data gap provides a major reason for laboratory measurements of the MSPEC response for specific crystals of interest.

The term dΩ/dA is determined by the crystal curvature and spectrometer geometry. It is the solid angle, seen from the source, that maps into a differential area element on the detector if the crystal behaved as a mirror. dΩ/dA was calculated as a function of photon energy (Bragg angle) using geometric formulas.

The last three terms in Eq. 1 are properties of the gated MCP framing camera; for the other detectors (x-ray CCD, x-ray film, and image plates), these terms would be replaced. M is the photoelectric efficiency of the MCP in units of secondary electrons per eV of photon energy. Based on previous work, we take M to be proportional to the x-ray absorption coefficient of the leaded MCP glass.[9] P is the relative efficiency of the MCP as a function of incident angle. Based on previous work, P = 1/sin(δ), where the angle δ is the quadrature sum of the MCP pore bias angle (8 degrees for our framing cameras) and the x-ray incidence incidence with respect to the MCP normal;[10] true for MCPs with pores angled perpendicular to diffraction direction. The flat-field correction F is the position-dependent variation in MCP gain for a fast gate pulse propagating across the MCP. It is determined from separate laser shots that uniformly illuminate the MCP with x-rays during the gate time.

To illustrate the MSPEC response, we consider the case of the E1 geometry with a PET crystal, for which the 2d spacing is 8.74 angstroms. The response for the E3 geometry with CsAP is similar, but with a different energy scale. For the integrated reflectivity of PET we use $R(E) = 0.106\,E^{0.58}$ mr[11], with *E* in keV,

recognizing that this may not be accurate for our bent crystal. The geometric contribution to the crystal response dΩ/dA is plotted in Fig. 2 for the E1 geometry, and the complete crystal response G(E) is shown in Fig. 3.

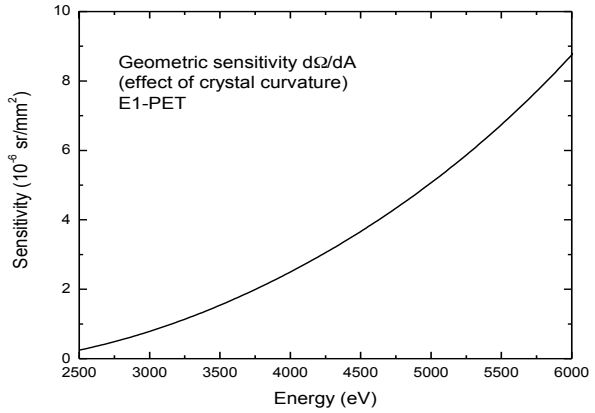

FIG. 2. Geometric contribution to the crystal response for the E1 geometry.

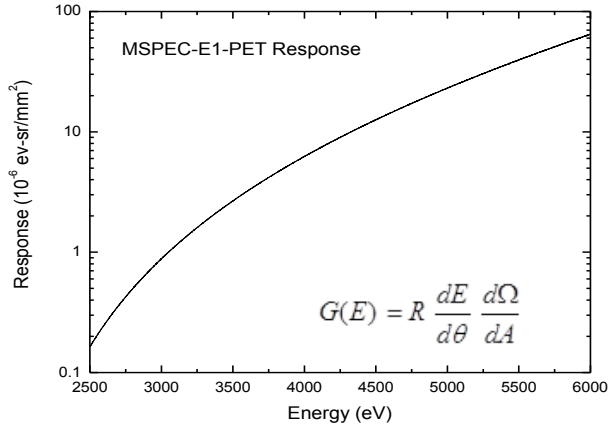

FIG. 3. Crystal response G(E) for PET in the E1 geometry.

The x-ray attenuation coefficient for the MCP glass was calculated using attenuation coefficients for silicon, oxygen, and lead combined according to the composition previously reported,[9] and measurements of similar plates at other facilities have also been consistent with calculations of this type.[9] For measurements at energies above the lead M-edges (2484, 2586 eV),[18] the response is particularly smooth. The dependence of the MCP response on incident angle is plotted in Fig. 4 as a function of x-ray energy, which determines the incident angle through Bragg's law and the MSPEC geometry.

A cooled, back-illuminated CCD detector with 1340 x 1300 20-μm pixels was used for some of the laboratory calibration measurements.[12] Its efficiency is determined by transmission of x-rays through the dead layer on the surface, combined with the probability of x-ray absorption within the depletion depth. The calculated quantum efficiency for the CCD detector used in the present work is shown in Fig. 5. Unlike the MCP, the absolute sensitivity of the CCD in pixel readout units per eV of deposited energy is known.

For some laser-plasma experiments, and for some calibration measurements discussed below, the MCP framing camera was replaced with a Fuji image plate (IP) of type BAS-TR. This type of IP is uncoated and sensitive to soft x-rays. Unlike the MCP, it has an approximately constant response as a function of deposited x-ray energy over the x-ray energy range of interest here.[13] However the absolute sensitivity of IP depends on the scanning parameters and is not well determined. Also, X-ray sensitive DEF and BIOMAX film have been used with the MSPEC in some laser-plasma experiments. The properties of these types of film have been published elsewhere[14,15] and are not discussed in this work.

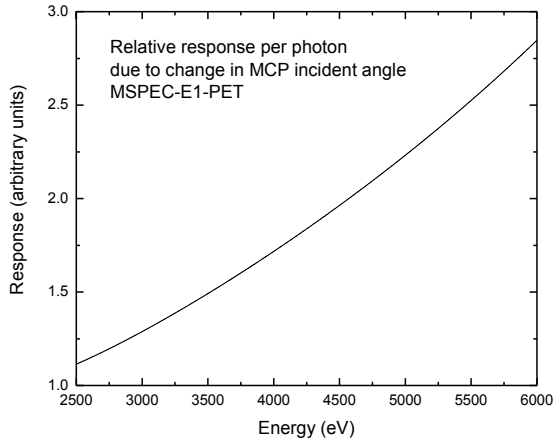

FIG. 4. Variation of MCP response with incident angle, plotted vs. photon energy for the MSPEC-E1 geometry and PET crystal.

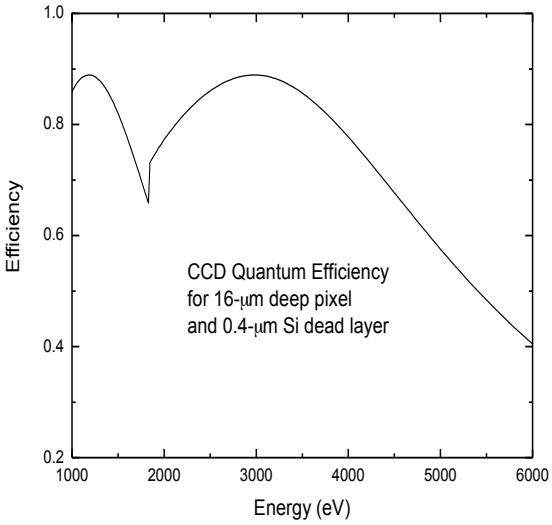

FIG. 5. Quantum efficiency of the CCD detector over the range of interest for the present work.

IV. MEASURED MSPEC RESPONSE

The MSPEC response was measured with a laboratory x-ray source to verify our model of the response, reduce the uncertainty in the integrated reflectivity of the crystal, and check the response of different detector types. The x-ray source used for the response measurements, typically known as a Manson source, has a flat anode that is viewed symmetrically at 45 degrees in two directions.[16] In one direction, x-rays were monitored with a 0.5-mm thick silicon detector that counted photons and provided a measure of the source emission spectrum and intensity.[17] The MSPEC viewed the source from the other direction, where the emission is expected to be identical by symmetry. Identical filters

were installed in both arms to adjust the incident spectrum and intensity. The setup is shown in Fig. 6.

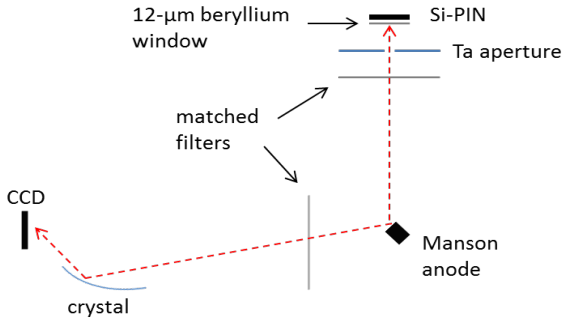

FIG. 6. Experimental arrangement for crystal calibration with the CCD detector.

The CCD, image plate, and MCP detectors were located at the detection plane as shown in Fig. 1. The Manson source anode was located at one focus of the MSPEC ellipse, the same place as the target in laser experiments. The ~1-mm diameter x-ray source is demagnified by the elliptical geometry, but still sets the instrumental resolving power $E/\Delta E \sim 300$.[4] Of the 3 detector types, the CCD is best for measuring the crystal response G(E): its sensitivity is known fairly well and its response is linear, i.e. output counts are proportional to deposited photon energy.

Fig. 7 shows examples of spectra obtained in the silicon detector with tin (Sn) and titanium (Ti) anodes. They were obtained in 500s with a 300μm diameter tantalum aperture at a distance of 61.5 cm from the x-ray source.

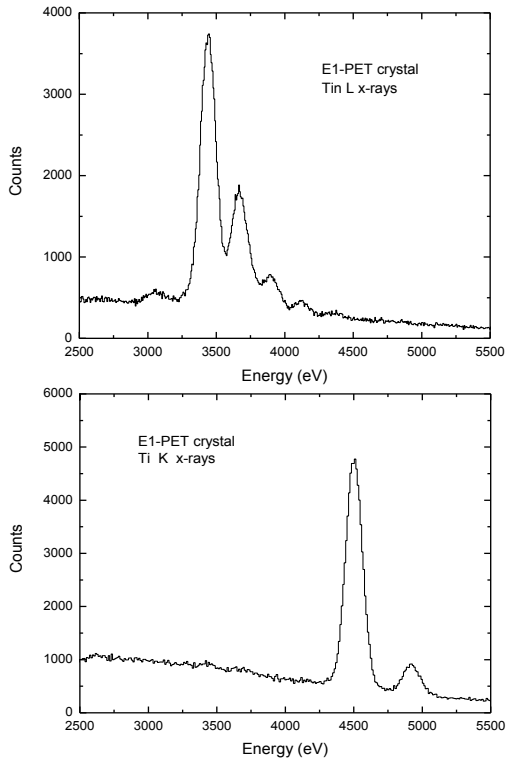

FIG. 7. Spectra obtained in the silicon detector from tin (top) and Ti (bottom) anodes, showing tin L, Ti K-α and K-β lines.

In Fig. 7, the 4 peaks in the Sn spectrum are L x-ray lines, and the two peaks in the Ti spectrum are K x-rays. The Sn x-rays were filtered with 26 μm of polypropylene, and the Ti x-rays were filtered with 50 μm of Ti. The intensities of the x-ray lines were determined by approximating the bremsstrahlung background with a smooth curve, and subtracting it. The peaks were then fitted to Gaussians. After small corrections for dead time and the efficiency of the silicon detector in this energy range, this gives the absolute filtered emission rate of these lines.

Fig. 8 shows sample images from the MSPEC with a PET crystal in E1 geometry as recorded with the CCD. The images show x-ray lines from Sn and Ti as well as bremsstrahlung background. The Sn and Ti spectra were obtained by averaging over a band of pixels in the direction perpendicular to the dispersion direction, and intensities of the x-ray lines were determined after subtraction of bremsstrahlung background. Correcting for the CCD efficiency (see Fig. 5) gives the (energy-dependent) response of the crystal G(E). The calculated and measured crystal response are compared in Fig. 9.

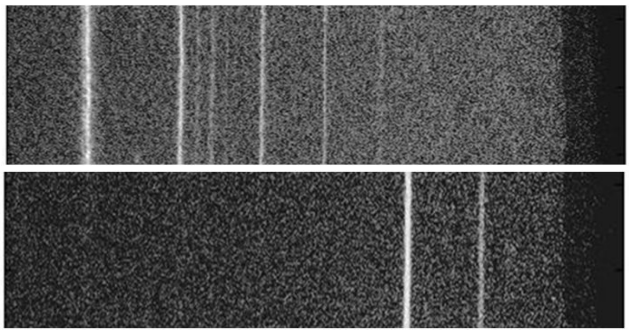

FIG. 8. CCD images for tin (top) and titanium (bottom) showing characteristic x-ray lines and bremsstrahlung background obtained with a PET crystal. Energy increases from left to right. The spectra are cut off on the high-energy side by the end of the crystal.

The calculation and measurements of the MSPEC response for CsAP crystals in the E3 geometry are similar to those for PET above, except for the different energy range. The CsAP measurements were done with a silver anode in the Manson source. The silver L x-rays span the energy range from 2980 to 3520 eV, but only the first of these lines is (just barely) in the range of the crystal. However, the K x-rays from silicon, sulfur, and chlorine contaminants on the anode provided useful calibration lines that spanned the energy range of the crystal, as can be seen in Fig. 10. The contaminants are attributed to sputtering of material from insulators in the Manson source. For longer exposures, the bremsstrahlung continuum radiation provides a map of the reflectivity of the crystal surface

The absolute MSPEC crystal response as measured with the CCD detector at the Kα energies of silicon, sulfur, and chlorine is shown in Fig. 11. The calculated crystal response is shown as the solid line in Fig. 11. It has been normalized to the data for display purposes, so only the shape (i.e., primarily the slope) is significant. Since we do not have good information on the CsAP reflectivity in this energy range, the crystal response was calculated assuming a constant integrated reflectivity. The measurements shown in Fig. 11 suggest that a better reflectivity model would be valuable; a power-law integrated reflectivity of the form $R = aE^b$ (with b=1.2 determined by best fit to this data).

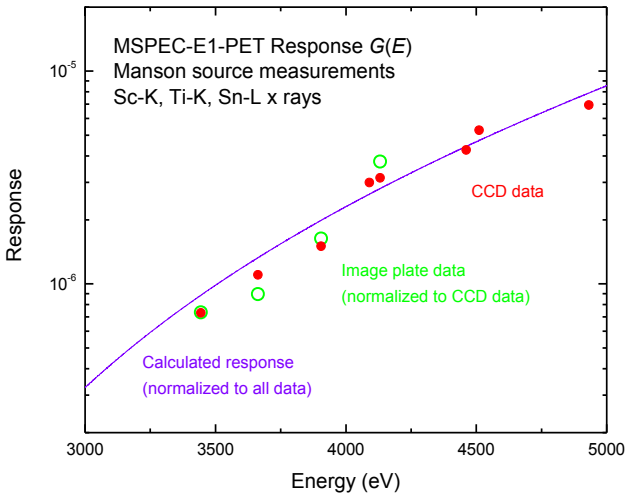

FIG. 9. MSPEC crystal response for PET crystal, E1 geometry. Solid points are absolute values from multiple measurements with the CCD detector, averaging together data taken at 5, 6, 7 and 8 kV anode voltages on the Manson source. The different source voltages produce different absolute and relative x-ray line intensities. The four open circles are measurements with Sn x-rays obtained with an IP; an overall normalization has been applied to these to match the CCD data, so only the slope of the IP data is significant. The solid curve is the calculated MSPEC crystal response normalized to the measurements.

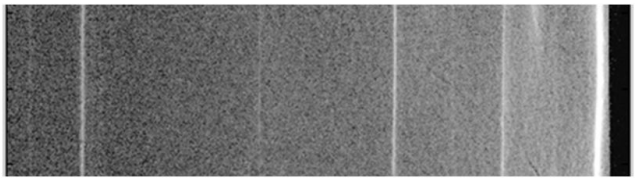

FIG. 10. Example of a CCD image obtained with a CsAP crystal in the E3 geometry. The four brightest lines are from left to right Si Kα, S Kα, Cl Kα, and Ag L.

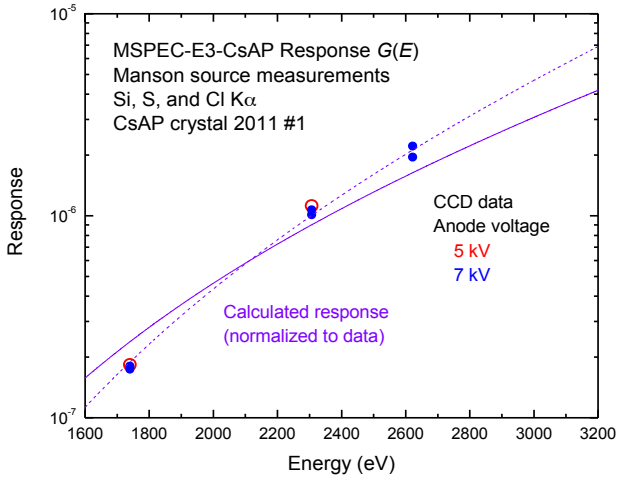

FIG. 11. MSPEC crystal response for CsAP crystal, E3 geometry. Solid points are absolute values from multiple measurements with the CCD detector, two at 7 kV anode voltage and one at 5 kV, for which the highest energy line was not measurable. The solid curve is the calculated MSPEC crystal response, with constant integrated reflectivity determined by best fit to the data. The dashed curve uses a power-law integrated reflectivity $R = aE^b$, with b=1.2 determined by best fit to the data.

V. SUMMARY

We have determined the energy-dependent response of an elliptical Bragg-crystal spectrometer by calculation and measurement, including the separate contributions of the crystal and two different detectors. Measurements with a laboratory x-ray source validate the model for the crystal response, and provide corrections for the poorly known integrated reflectivity of the bent crystals. The measurements also validate the models used for the response of the image plate detectors, by comparison to the better known response of a CCD detector. Combined with instrument-specific response data for specific microchannel-plate detectors, these results enable more accurate, relative spectral intensity measurements for time-resolved as well as time-integrated x-ray emission from laser produced plasmas.

ACKNOWLEDGMENTS

This work was performed under the auspices of the U.S. Department of Energy by Lawrence Livermore National Laboratory under Contract DE-AC52-07NA27344.

REFERENCES

1. H.R. Griem, *Principles of Plasma Spectroscopy* (Cambridge Univ. Press, Cambridge, England, 1997).
2. R.F. Heeter *et al.*, *Phys. Rev. Lett.* **99**, 195001 (2007).
3. M.J. May, R. Heeter and J. Emig, *Rev. Sci. Instrum.* **75**, 3740 (2004).
4. R. F. Heeter, J. A. Emig, K. B. Fournier, S. B. Hansen, M. J. May, and B. K. F. Young, Rev. Sci. Instrum. 75, 3762 (2004).
5. P. W. Lake, J. E. Bailey, G. A. Rochau, T. C. Moore, D. Petmecky, and P. Gard, Rev. Sci. Instrum. 75, 3690 (2004). See also S. G. Anderson, R. F. Heeter, R. Booth, J. Emig, S. Fulkerson, T. McCarville, D. Norman, and B. K. F. Young, Rev. Sci. Instrum. 77, 063115 (2006).
6. L.R. Benedetti et al., Rev. Sci Instrum. 83, 10E135 (2012).
7. X-ray Database, Center for X-Ray Optics, http://www.cxro.lbl.gov, using data from ref [9] below.
8. G.V. Brown et al., Rev. Sci. Instrum. 79, 10E309 (2008).
9. G. A. Rochau et al., Rev. Sci. Instrum. 77, 10E323 (2006); also S. Hubert, J. L. Dubois, D. Gontier, G. Lidove, C. Reverdin, G. Soullie, P. Stemmler, and B. Villette, Rev. Sci. Instrum. 81, 053501 (2010).
10. O. L. Landen, A. Lobban, T. Tutt, P. M. Bell, R. Costa, D. R. Hargrove, and F. Ze, Rev. Sci. Instrum. 72, 709 (2001).
11. B.L. Henke, E.M. Gullikson and J.C. Davis, Atomic Data and Nuclear Data Tables 54, 181-342 (1993).
12. Princeton Instruments 1340 × 1300 back-illuminated imaging array.
13. M.J. Haugh, J. Lee, E. Romano and M.B. Schneider, Proc. SPIE 8850, 885007 (2013), B.R. Maddox, et al., Rev. Sci. Instrum. 82, 023111 (2011) and A.L. Meadowcroft, C.D. Bentley and E.N Stott, Rev. Sci. Instrum. 79, 113102 (2008).
14. B.L. Henke, J.Y. Uejio, G.F. Stone, C.H. Dittmore and F.G. Fujiwara, J. Opt. Soc. Am. B 3, 1540 (1986).
15. J.P. Knauer et al., Rev. Sci. Instrum. 77, 10R331 (2006).
16. Manson® X-Ray source manufactured by Austin Instruments, 10 Temple Street, Reading, MA 01867-2830.
17. Amptek 0.5-mm thick silicon PIN detector with 12.5-μm Be window.
18. J.A. Bearden and A.F. Burr, Rev. Mod. Phys. 39, 125 (1967) as quoted in X-Ray Data Booklet (LBNL/Pub-490 Rev 2, January 2001).